

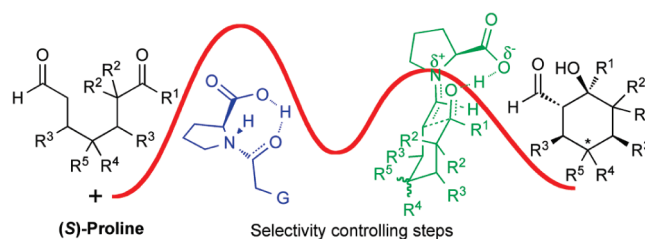
Asymmetric Intramolecular Aldol Reactions of Substituted 1,7-Dicarbonylic Compounds. A Mechanistic Study

F. J. S. Duarte,[†] E. J. Cabrita,[†] G. Frenking,[‡] and A. Gil Santos^{*†}

[†]REQUIMTE, CQFB, Departamento de Química, Faculdade de Ciências e Tecnologia (FCT), Universidade Nova de Lisboa, 2829-516 Caparica, Portugal, and [‡]Fachbereich Chemie, Philipps-Universität Marburg, Hans-Meerwein Strasse, 35032 Marburg, Germany

ags@dq.fct.unl.pt

Received January 12, 2010



The diastereo- and enantioselectivity obtained experimentally by List on the proline-catalyzed intramolecular aldol reaction of substituted 1,7-dicarbonylic compounds was accurately predicted using density functional theory methods at the B3LYP/6-31++G** level. A polarizable continuum model was used to describe solvent effects. The theoretical data agree in good extension with List's experimental results, both in enantioselectivity and diastereoselectivity, and allow for the confirmation of our previous rationalization of the main factors contributing to the reaction selectivity. While the enantioselectivity results from an important electrostatic contact between the forming alkoxide group and the proline moiety, the calculated diastereoselectivity results from several steric contacts that can be established between the different substituents and from their relative orientation in respect to the ring conformation. However, for dialdehydes that can originate two diastereomeric enamine intermediates, the proline attack and the immonium formation steps can also be of major importance in the rationalization of the final reaction selectivity, as is the case in two of the six studied systems. The obtained data allows for a full rationalization of the known experimental systems as well as for the extrapolation to new ones with variable substitution at the carbonylic chain.

Introduction

Aldol reactions are key carbon–carbon bond-forming reactions that have tremendous synthetic utility and are often the platform of choice to examine new organocatalysts. The versatility as well as the synthetic significance of the

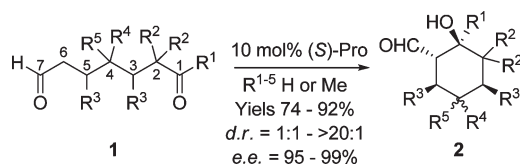
transformation has been extensively studied.^{1–11} In its intramolecular approach, aldol reactions of dialdehydes, keto-aldehydes and diketones are very efficient ways to prepare five-, six-, and seven-membered rings (Scheme 1).^{10,12,13}

Although amine-catalyzed non-asymmetric *enol*_{exo} aldolizations are relatively common and catalytic asymmetric *enolendo* aldolizations have been known for three decades,^{14–17}

(1) Amedjkouh, M. *Tetrahedron: Asymmetry* **2005**, *16*, 1411–1414.
(2) Cordova, A.; Zou, W.; Ibrahim, I.; Reyes, E.; Engqvist, M.; Liao, W.-W. *Chem. Commun.* **2005**, 3586–3588.
(3) Dalko, P. I.; Moisan, L. *Angew. Chem., Int. Ed.* **2004**, *43*, 5138–5175.
(4) Guillena, G.; Nájera, C.; Ramón, D. J. *Tetrahedron: Asymmetry* **2007**, *18*, 2249–2293.
(5) List, B. *Tetrahedron* **2002**, *58*, 5573–5590.
(6) List, B. *Chem. Commun.* **2006**, 819–824.
(7) Mukaiyama, T. *Org. React.* **1982**, *28*, 203–331.
(8) Northrup, A. B.; Mangion, I. K.; Hetteche, F.; MacMillan, D. W. C. *Angew. Chem., Int. Ed.* **2004**, *43*, 2152–2154.
(9) Notz, W.; Tanaka, F.; Barbas, C. F. *Acc. Chem. Res.* **2004**, *37*, 580–591.

(10) Pidathala, C.; Hoang, L.; Vignola, N.; List, B. *Angew. Chem., Int. Ed.* **2003**, *42*, 2785–2788.
(11) Kurteva, V. B.; Afonso, C. A. M. *Tetrahedron* **2005**, *61*, 267–273.
(12) Kurteva, V. B.; Afonso, C. A. M. *J. Mol. Catal. A: Chem.* **2005**, *234*, 159–167.
(13) Uli, K. *Angew. Chem., Int. Ed.* **2005**, *44*, 2186–2188.
(14) Eder, U.; Sauer, G.; Weichert, R. *Angew. Chem., Int. Ed.* **1971**, *10*, 496–497.
(15) Eder, U.; Sauer, G.; Weichert, R. German Patent DE2014757, **1971**.
(16) Hajos, Z. G.; Parrich, D. R. German Patent DE2102623, **1971**.
(17) Hajos, Z. G.; Parrish, D. R. *J. Org. Chem.* **1974**, *39*, 1615–1621.

SCHEME 1. General Intramolecular Aldol Reaction

SCHEME 2. Proline-Catalyzed Enantioselective 6-*enolexo* Aldolizations of Dicarbonyl Compounds¹⁰

the first catalytic asymmetric *enolexo* aldolizations were developed only recently by List and co-workers for several 1,7-dicarbonyl compounds.^{10,18} It was observed that a variety of structures of type **1**, on treatment with a catalytic amount of (*S*)-proline, furnished *anti*-aldols **2** with excellent enantioselectivity (Scheme 2). Differently substituted heptanedials can be used in the reaction, but monosubstitution at the C4 position induces an unexpected and not explained effect on the outcome stereoselectivity of the product, resulting in a complex mixture of diastereomers. The generalized use of this reaction in aldol intramolecular cyclizations depends on the rationalization of this experimental data and on its extrapolation to the effect of other substituents in the molecular chain.

It is common that amino acids as proline or proline derivatives are used as catalysts in intramolecular aldol reactions of dicarbonyl compounds.^{10,11,14,17,19–24} In the past years the mechanism of this reaction has been intensively studied by theoretical approaches.^{25–31} Houk has proposed a mechanism for 6-*enolexo* aldolizations of diketones,^{25–29} and on the basis of Houk's results, List proposed an empirical model for the 6-*enolexo* variant.¹⁰ In both cases, it is accepted that the mechanism involves the formation of an enamine intermediate, followed by a transition state with concerted C–C bond formation and proton transfer from the carboxylic acid group in the catalyst to the carbonyl acceptor in the substrate (Scheme 3).

(18) Mukherjee, S.; Yang, J. W.; Hoffmann, S.; List, B. *Chem. Rev.* **2007**, *107*, 5471–5569.

(19) Cohen, N. *Acc. Chem. Res.* **1976**, *9*, 412–417.

(20) Danishefsky, S.; Cain, P. *J. Am. Chem. Soc.* **1976**, *98*, 4975–4983.

(21) Itagaki, N.; Sugahara, T.; Iwabuchi, Y. *Org. Lett.* **2005**, *7*, 4181–4183.

(22) Kumar, I.; Bhide, S. R.; Rode, C. V. *Tetrahedron: Asymmetry* **2007**, *18*, 1210–1216.

(23) Limbach, M. *Tetrahedron Lett.* **2006**, *47*, 3843–3847.

(24) Nagamine, T.; Inomata, K.; Endo, Y.; Paquette, L. A. *J. Org. Chem.* **2007**, *72*, 123–131.

(25) Allemann, C.; Gordillo, R.; Clemente, F. R.; Cheong, P. H. Y.; Houk, K. N. *Acc. Chem. Res.* **2004**, *37*, 558–569.

(26) Bahmanyar, S.; Houk, K. N. *J. Am. Chem. Soc.* **2001**, *123*, 12911–12912.

(27) Bahmanyar, S.; Houk, K. N. *J. Am. Chem. Soc.* **2001**, *123*, 11273–11283.

(28) Clemente, F. R.; Houk, K. N. *Angew. Chem., Int. Ed.* **2004**, *43*, 5766–5768.

(29) Clemente, F. R.; Houk, K. N. *J. Am. Chem. Soc.* **2005**, *127*, 11294–11302.

(30) Duarte, F. J. S.; Cabrita, E. J.; Frenking, G.; Santos, A. G. *Eur. J. Org. Chem.* **2008**, 3397–3402.

(31) Duarte, F. J. S.; Cabrita, E. J.; Frenking, G.; Santos, A. G. *Chem.—Eur. J.* **2009**, *15*, 1734–1746.

Recently, we envisaged a theoretical study³⁰ aiming at the validation of the empirical model proposed by List,¹⁰ and we were able to show that the experimental results obtained for the cyclization of 1,7-heptanedial, catalyzed by (*S*)-proline, can indeed be rationalized by the TS in Figure 1. Steric and electrostatic interactions in the transition structure were identified as the main factors that contribute to the calculated selectivities. While the high calculated enantioselectivities mainly originate from different electrostatic interactions between O1 and HC11, the calculated diastereoselectivities result from the equatorial versus axial orientation of the proline moiety in the TSs (Figure 1).

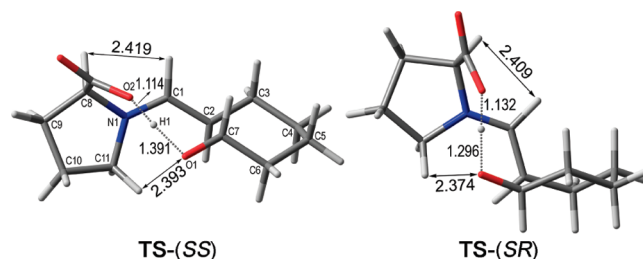
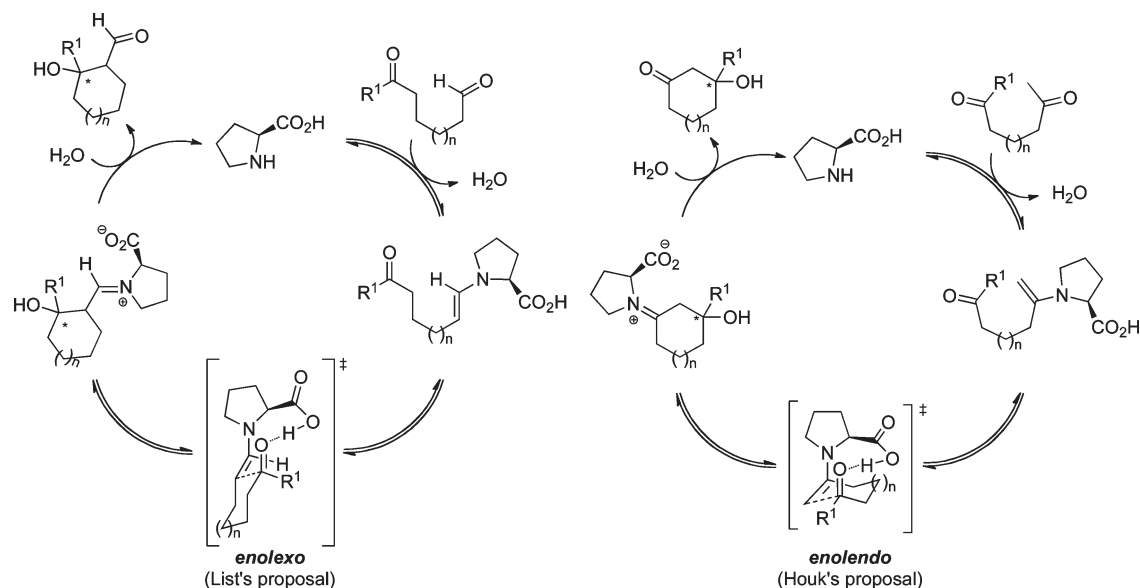


FIGURE 1. Diastereomeric transition-state structures for the cyclization of heptanedial catalyzed by (*S*)-proline.³⁰

As already mentioned above, List and co-workers also experimentally studied other 1,7-dicarbonyl compounds with one or two methyl substituents in different positions of the carbon chain (Scheme 2). It was observed that the diastereoselectivity is extremely affected when a methyl group is added to the C4 carbon atom in the chain, while minor changes were observed when methyl groups are simultaneously added to the C3 and C5 carbon atoms (*meso* structure). In this paper we substantially extend our previously validated model, by showing that it is also able to efficiently rationalize the experimental results obtained for the substituted structures. Almost all known data fits quite well with the proposed model, allowing its future extrapolation to systems with other types of functionalizations.

Results and Discussion

List and co-workers reported¹⁰ that a variety of achiral hepta-dicarbonyl compounds (**3–8**), on treatment with a catalytic amount of (*S*)-proline, furnished *anti*-aldol structures (**9–14**) with excellent enantioselectivity (Table 1). Differently substituted heptanedials can be used in the reaction. However, substituents in the C3 or C4 positions have unfavorable effects on the outcome stereoselectivity of the product. Our previous theoretical studies on the intramolecular aldol reaction of heptanedial³⁰ suggest that the stereoselectivity of the reaction depends on the transition-state conformation of the intramolecular cyclization step (Figure 1), as a result of different steric and electrostatic contacts established inside the TS structure. Substituent groups in the hepta-dicarbonyl structure can change these contacts or induce new ones, thus changing the relative activation energies of the TS structures as well as the final observed selectivities. As stated by List,¹⁰ explaining the stereoselectivity is difficult without calculating the relative energies of all reasonable transition states. Thus, on the basis of our previous work,³⁰ we now analyze the predicted effects of

SCHEME 3. Proposed Mechanisms for *enolexo*¹⁰ and *enolendo*^{25–29} Intramolecular Adol Reactions Catalyzed by ProlineTABLE 1. Proline-Catalyzed Enantioselective 6-*enolexo* Aldolizations of Dicarbonyl Compounds¹⁰

Dicarbonyl	Product	Yield (%)	<i>e.e.</i> (%)	<i>d.r.</i> (%)
		95	99	90.9 : 9.1
		74	98	> 95.2 : 4.8
		75	97	> 95.2 : 4.8
		76	> 95, 89, 75, 8	66.7:15.2: 15.2:3.0
		88	99, 75	50 : 50
		92	99	66.7 : 33.3

several chain substituents and compare them with the experimental results obtained by List, which are summarized in Table 1. The obtained data allow for a full rationalization of the known experimental systems as well as for the extrapolation to new ones with variable substitution at the carbonylic chain.

In our previous work³⁰ we used a basis set without diffuse functions (6-31G**). The present work indicates that diffuse functions have to be introduced (6-31++G**), in order to properly describe the formation of negative charges and several important electrostatic contacts in the TS structures.

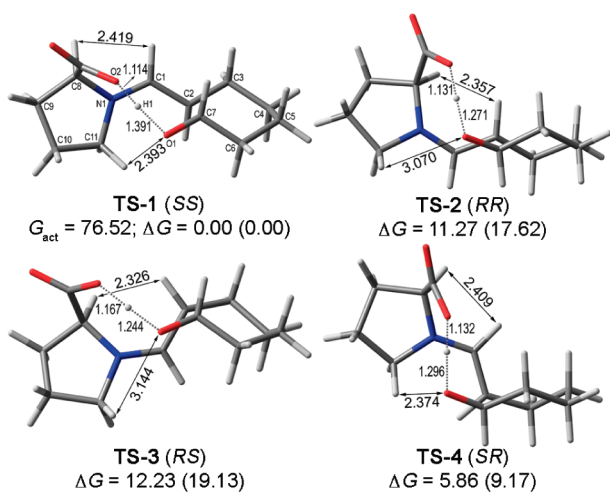


FIGURE 2. Calculated transition-state structures for the cyclization of **3** to **9** catalyzed by (*S*)-proline. Scaled ($sf = 0.6395$) relative transition-state Gibbs energies in dichloromethane (kJ mol^{-1}). Nonscaled values are in parentheses. For a detailed discussion on the selectivities calculated for the reaction of compound **3**, see ref 30.

With the previous basis set a bad fitting between the theoretical and the experimental data was obtained. We also observed that the smaller basis set affords results that do not fit the recent experimental results by Meyer and collaborators,³² while the theoretical results obtained with the larger basis set properly fit those results, as discussed later. Because the calculated data indicate that the present level of theory overestimates the predicted diastereoselectivities, we introduced a scaling factor (sf), obtained by the comparison of the theoretical values found for the reaction of dialdehyde **3** and the experimental known results (see Figure 2 and Table 2). The same scaling factor was used to normalize the energy values calculated throughout this manuscript.

The rationalization of the calculated selectivities in the cyclization of compound **3** was discussed elsewhere³⁰ and will be not repeated here. Nevertheless, a revision of the main concepts will be made during the discussion of the selectivities calculated for the cyclization of structure **4**.

The first step in the mechanism of the intramolecular aldol reaction catalyzed by (*S*)-proline involves the formation of an enamine intermediate (Scheme 3). With dialdehydes **3** and **5** the first step has no relevance on the final selectivity outcome and will not be considered in the discussion. On the other hand, for structures **4**, **6**, **7**, and **8** it is necessary to take in account the kinetics of the first step, which potentially generates enamine intermediates with different structures and can lead to different final products (**4** and **8**) or to final products with different configurations (**6** and **7**).

(*S*)-Proline can react with dialdehyde **4** at two different centers but the process is simplified, as the enamine formation is possible at only one of them (Scheme 4). Enamine **15** can originate four diastereomers of compound **10**, via four different TSs (more TS conformations were calculated, but their energy is too large to be relevant). The TS relative energies are given in Table 3, whereas Figure 3 shows the respective 3D transition structures.

TABLE 2. Relative Transition-State Gibbs Energies (kJ mol^{-1} , $sf = 0.6395$),^a Enantioselectivities, and Diastereoselectivities in the Intramolecular Aldol Reaction of Dialdehyde **3**, in Dichloromethane^b

transition state	B3LYP/6-31++G**// B3LYP/6-31G** ($sf = 0.6395$)		ref 10		
	ΔG (kJ mol^{-1})	ee (%)	dr (%)	ee (%)	dr (%)
TS-1 (<i>SS</i>) <i>anti</i>	0.00 (0.00)	97.9 (99.8)	90.9 (97.5)	99.0	90.9
TS-2 (<i>RR</i>) <i>anti</i>	11.27 (17.62)	99.8	85.8		
TS-3 (<i>RS</i>) <i>syn</i>	12.23 (19.13)	85.8	9.1		
TS-4 (<i>SR</i>) <i>syn</i>	5.86 (9.17)	(96.5)	(2.5)		9.1

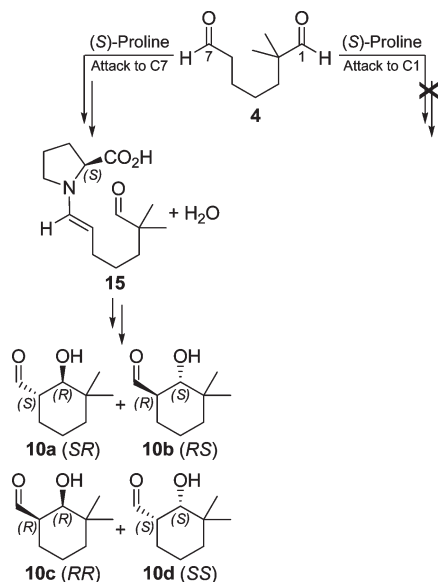
^aCalculated dr of the *anti* structures forced to fit the experimental value. ^bNon-scaled values are in parentheses. *Syn/anti* refers to the configuration of the final products, as defined by List.¹⁰

The TS structures in Figure 3 are very similar to the TS structures previously proposed for the cyclization of heptanedial (Figure 2).³⁰ In all structures the hydrogen bond between the carboxylic acid group and the forming alkoxide oxygen atom (O1–HC11) induces the formation of low-energy chair conformations as well as intramolecular acid catalysis. This is a characteristic interaction observed in enamine-mediated aldol reactions catalyzed by (*S*)-proline and is mandatory for the stabilization of the negative charge formed on the carbonyl oxygen atom during the cyclization step.²⁸ In dichloromethane (DCM) the activation energy of TS-5 ($79.51 \text{ kJ mol}^{-1}$) is very similar to the value calculated for TS-1 ($76.52 \text{ kJ mol}^{-1}$) (Figure 2), which indicates that the methyl substituents only slightly disturb the formation of the TS chair conformations. TS-5 (*SR*) is $11.24 \text{ kJ mol}^{-1}$ less energetic than TS-6 (*RS*), whereas TS-8 (*SS*) is 2.36 kJ mol^{-1} more stable than its enantiomer TS-7 (*RR*).

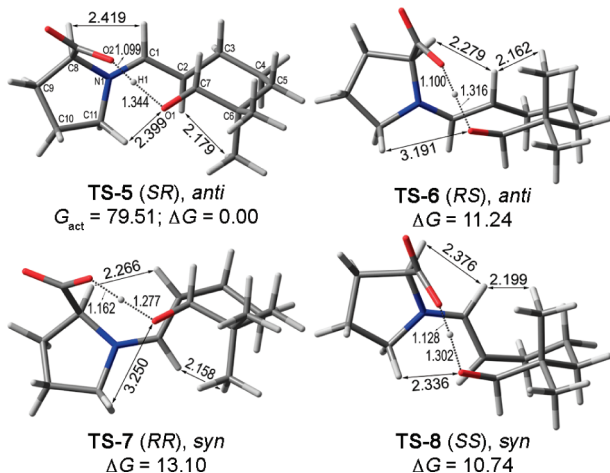
The main factors conditioning the relative stability of the TS structures in Figure 3 (TS-5 to TS-8) are similar to those found in TS structures TS-1 to TS-4 (Figure 2), with the O1–HC11 electrostatic interaction defining the calculated enantioselectivity. The introduction of the two methyl groups induces a large energy difference in TS-8 (about 5 kJ mol^{-1}), when compared with its analogous TS-4, but the relative energy of TS-6 is almost unchanged (0.03 kJ mol^{-1} (compared with TS-2), and the relative energy of TS-7 only increases by about 0.8 kJ mol^{-1} (compared with TS-3). The calculated energy value for TS-8 results from two factors: the axial orientation of the enamine group, which induces a steric contact with the axial methyl substituent, and the *syn* orientation of the carboxyl group in relation to the axial methyl substituent. When these two conditions are met (structure TS-8), the bulkiness of the enamine moiety is maximized as well as its steric interaction with the axial methyl substituent. This effect is responsible for the large diastereoselectivity improvement observed for the dialdehyde **4** when compared with heptanedial **3** and for the strong decrease in the enantioselectivity calculated between enantiomers TS-7 and TS-8.

Because of the C4 dimethyl substitution of dialdehyde **5**, the nucleophilic attack of (*S*)-proline at either one or the other carbonyl groups originates only one enamine intermediate. This compound undergoes cyclization via four transition states, leading to four diastereomers of compound **11** (Figure 4). The relative energies of the different TSs are given in Table 4, whereas Figure 4 shows the respective transition structures.

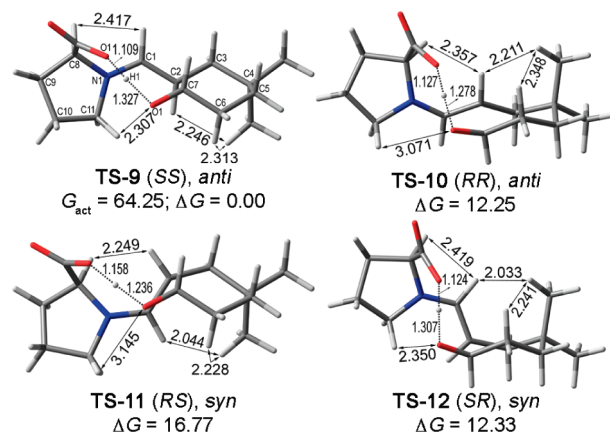
(32) Zhu, H.; Clemente, F. R.; Houk, K. N.; Meyer, M. P. *J. Am. Chem. Soc.* **2009**, *131*, 1632–1633.

SCHEME 4. Proposed Mechanism for the Intramolecular Aldol Reaction of Dialdehyde 4 Catalyzed by (*S*)-proline

TABLE 3. Relative Transition-State Gibbs Energies (kJ mol^{-1} , $\text{sf} = 0.6395$), Enantioselectivities, and Diastereoselectivities in the Intramolecular Aldol Reaction of Dialdehyde 4, in Dichloromethane

transition state	B3LYP/6-31++G**//B3LYP/6-31G** (sf = 0.6395)			ref 10	
	ΔG (kJ mol^{-1})	ee (%)	dr (%)	ee (%)	dr (%)
TS-5 (<i>SR</i>) <i>anti</i>	0.00	97.9	98.2	98	> 95.2
TS-6 (<i>RS</i>) <i>anti</i>	11.24				
TS-7 (<i>RR</i>) <i>syn</i>	13.10				
TS-8 (<i>SS</i>) <i>syn</i>	10.74	44.3	1.8		< 4.8


FIGURE 3. Calculated transition-state structures for the cyclization of 4 to 10 catalyzed by (*S*)-proline. Relative transition-state Gibbs energies ($\text{sf} = 0.6395$) in dichloromethane (kJ mol^{-1}).

The activation energy in the cyclization of compound 5 is substantially lower ($64.25 \text{ kJ mol}^{-1}$) than the value calculated for compound 3 ($76.52 \text{ kJ mol}^{-1}$) (Figure 2), because compound 3 prefers to adopt a linear conformation and any change to this ideal situation implies a strong increment in the steric energy. Compound 5, on the other hand, due to its

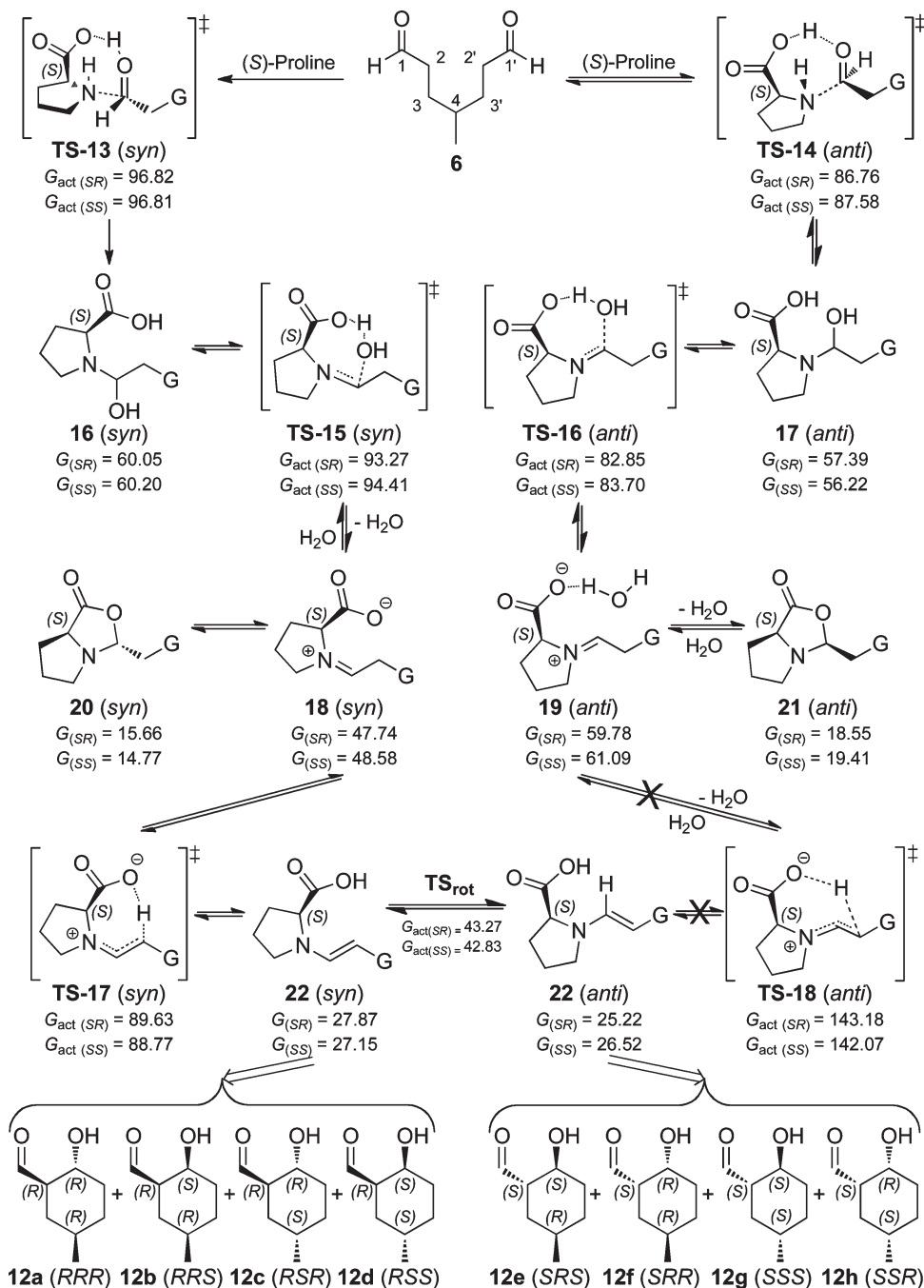

FIGURE 4. Calculated transition-state structures for the cyclization of 5 to 11 catalyzed by (*S*)-proline. Relative transition-state Gibbs energies (scaling factor = 0.6395) in dichloromethane (kJ mol^{-1}).
TABLE 4. Relative Transition-State Gibbs Energies (kJ mol^{-1} , $\text{sf} = 0.6395$), Enantioselectivities, and Diastereoselectivities in the Intramolecular Aldol Reaction of Dialdehyde 5, in Dichloromethane

transition state	B3LYP/6-31++G**//B3LYP/6-31G** (sf = 0.6395)			ref 10	
	ΔG (kJ mol^{-1})	ee (%)	dr (%)	ee (%)	dr (%)
TS-9 (<i>SS</i>) <i>anti</i>	0.00				
TS-10 (<i>RR</i>) <i>anti</i>	12.25	98.6	99.2	98	> 95.2
TS-11 (<i>RS</i>) <i>syn</i>	16.77				
TS-12 (<i>SR</i>) <i>syn</i>	12.33	71.3	0.8		< 4.8

double substitution at C4, does not suffer such a large energy increment when the linear conformation is changed. This happens because the steric interactions that arise when the two extremes of the chain approach each other are in part compensated by the reduction of the steric repulsion between the methyl substituents and the main carbon chain (see Figure S1 in Supporting Information).

The four TS structures calculated for the cyclization of dialdehyde 5 (Figure 4) are similar to those obtained for dialdehydes 3 and 4 (Figures 2 and 3). The activation energy of TS-10 relative to TS-9 follows the same pattern observed in the previous discussed systems, indicating that, also in this case, the main factor conditioning the enantioselectivity is the O1-HC11 electrostatic contact. On the other hand, the calculations predict a strong energy increment for structures TS-11 and TS-12, in relation to TS-9. This is a result of the axial orientation of the enamine moiety, which induces important steric contacts with either one or the other axial methyl group in C4. As observed in the cyclization of dialdehyde 4, the energy increment is larger when the carboxyl group is orientated *syn* to the axial methyl substituent.

In contrast to the previously discussed structures, the reaction between dialdehyde 6 and (*S*)-proline can occur at two different carbonyl groups that lead to the formation of two diastereomeric enamine intermediates 22 (*SR:SS*) (Scheme 5), in conformational equilibrium between the *syn* and *anti* conformers. If the rate-limiting step is the cyclization step, all previous steps are irrelevant for the calculated stereoselectivity. Nevertheless, Houk predicted that the rate-limiting step can be the enamine formation,²⁸ while more

SCHEME 5. Proposed Mechanism for the Intramolecular Aldol Reaction of Dialdehyde 6 Catalyzed by (S)-Proline^a

^aFree energies in kJ mol^{-1} .

recently, on the basis of experimental results, Meyer suggested that the rate-limiting step has to precede the enamine formation.³² In accordance with Houk's proposal, the calculation of the structures in Scheme 5 with B3LYP/6-31G** predict the enamine formation as the rate-limiting step (see Supporting Information). Nevertheless, the introduction of diffuse functions (6-31++G**) changes this prediction, affording a result in agreement with Meyer's proposal. According to Scheme 5, the predicted rate-limiting step is the initial attack of the proline molecule, while the immonium formation is more stable by ca. 2.5 kJ mol^{-1} and the

enamine formation is more stable by ca. 7.5 kJ mol^{-1} . However, considering the similarity of values, one should be very careful in making final conclusions. We can only say, with good confidence, that the rate-limiting step is not the cyclization step, as it is around 30 kJ mol^{-1} more stable than the initial proline attack (Scheme 5 and Figure 5).

The attack of the proline molecule to the aldehyde can originate four isomers, depending on the reacting carbonyl and on the orientation of the aldehyde chain, in relation to the carboxyl group in the proline moiety (*syn/anti*). As expected, the *anti* structures are slightly more stable than

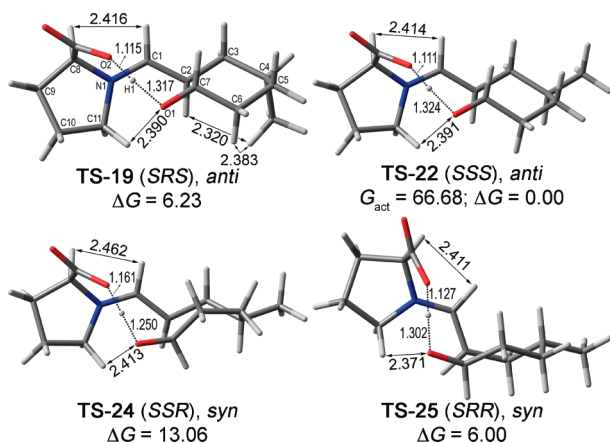


FIGURE 5. Calculated transition-state structures for the cyclization of **6** to **12** catalyzed by (*S*)-proline. Relative transition-state Gibbs energies (sf = 0.6395) in dichloromethane (kJ mol⁻¹).

the *syn* isomers as a result of different steric interactions between the aldehyde chain and the proline carboxyl group. Nevertheless, the formation of the enamine intermediate via the *anti* pathway will not occur, as it is a very energetic step (Scheme 5). Thus, all of the previous steps have to be reversible and the enamine formation has to occur via the *syn* pathway. The Seebach oxazolidinones **20** and **21**, experimentally observed in this type of reactions,^{33–36} are substantially more stable than compounds **18** and **19**, respectively, but we were not able to find TS structures for their interconversion, which means that they do not affect the pathways reversibility, in accordance with the experiment.³⁶ The attack of the proline molecule, on one or the other carbonyl group in the dialdehyde, seems to occur with no selectivity, leading to the two possible diastereomers of enamine **22** in a 50:50 ratio. Even if the rate-limiting step is the immonium or the enamine formation, this statement does not change, as these steps also predict very low selectivity (Scheme 5). Thus, the cyclization step can occur from enamines **22** (*SR* and *SS*), which are formed via two concurrent nonselective *syn* pathways and lead to opposite enantiomers of the final product **12**. The final calculated selectivity results from the two independent selectivity calculations on the cyclization step, pondered by the selectivity obtained in the proline addition step (TS-13 (*syn*) *SR* ⇒ (**12a**, **12b**, **12e**, **12f**) and TS-13 (*syn*) *SS* ⇒ (**12c**, **12d**, **12g**, **12h**)).

The relative energy values and selectivities calculated for the proline-catalyzed cyclization of compound **6** are given in Table 5, while four selected structures are presented in Figure 5 (extra data is available in Supporting Information). In Table 5, the values in italic were calculated considering the proline attack to the aldehyde as the rate-limiting step of the overall reaction, while the values in plain text were calculated considering that the selectivity results only from the cyclization step. From the comparison of these two sets of data, we

(33) Seebach, D.; Beck, A. K.; Badine, D. M.; Limbach, M.; Eschenmoser, A.; Treasurywala, A. M.; Hobi, R.; Prikoszovich, W.; Linder, B. *Helv. Chim. Acta* **2007**, *90*, 425–471.

(34) Orsini, F.; Pelizzoni, F.; Forte, M.; Sisti, M.; Bombieri, G.; Benetollo, F. *J. Heterocycl. Chem.* **1989**, *26*, 837–841.

(35) Zotova, N.; Franzke, A.; Armstrong, A.; Blackmond, D. G. *J. Am. Chem. Soc.* **2007**, *129*, 15100–15101.

(36) List, B.; Hoang, L.; Martin, H. J. *Proc. Natl. Acad. Sci. U.S.A.* **2004**, *101*, 5839–5842.

TABLE 5. Relative Transition-State Gibbs Energies (kJ mol⁻¹, sf = 0.6395), Enantioselectivities, and Diastereoselectivities in the Intramolecular Aldol Reaction of Dialdehyde **6**, in Dichloromethane^a

transition state	B3LYP/6-31++G**//B3LYP/6-31G** (sf = 0.6395)		ref 10		
	Δ <i>G</i> (kJ mol ⁻¹)	ee (%)	dr (%)	ee (%)	dr (%)
TS-19 (<i>SRS</i>) <i>anti</i>	6.23, <i>0.23</i>	99.7	<i>21.9</i>	95	15.2
TS-20 (<i>RRS</i>) <i>anti</i>	18.06	98.3	6.8		
TS-21 (<i>RRR</i>) <i>anti</i>	11.06, <i>5.06</i>	88.1	<i>52.5</i>		
TS-22 (<i>SSS</i>) <i>anti</i>	0.00	97.7	84.4	75	66.7
TS-23 (<i>RRS</i>) <i>syn</i>	14.07, <i>8.07</i>	<i>57.0</i>	<i>1.2</i>		
TS-24 (<i>SSR</i>) <i>syn</i>	13.06	20.1	0.7	8	3.0
TS-25 (<i>SRR</i>) <i>syn</i>	6.00, <i>0.00</i>	96.7	<i>24.4</i>		
TS-26 (<i>RSS</i>) <i>syn</i>	11.89	83.0	8.1	89	15.2

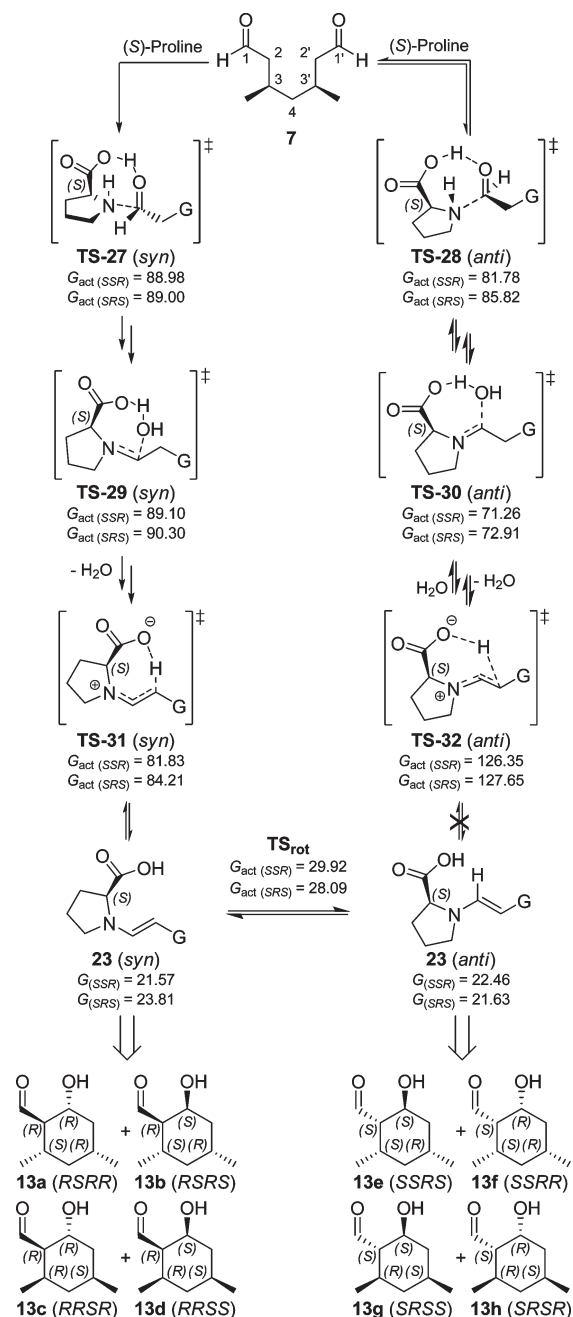
^aWith (italic) and without (plain text) accounting for the selectivity obtained in TS-13 (*syn* dr = 50.0:50.0).

conclude that the reaction pathway before the cyclization step is mandatory for the rationalization of the experimental diastereoselectivity. The calculated enantioselectivities, despite being slight overestimated, follow the same trend as the experimental values.

As was previously observed for the cyclization of compound **5**, the presence of a methyl group in position C4 of the dialdehyde chain substantially reduces the TS energy ($G_{\text{act}} = 66.68$ kJ mol⁻¹), as it helps at the formation of the reactive conformation. Also, and as discussed before, the electrostatic interaction between O1 and HC11 is still the main factor controlling the TS energies, as shown in Figure 5. With one exception (TS-24), the structures with this electrostatic contact are the most stable and account with more than 98% for the overall selectivity. TS-24 does not follow this trend because in order to avoid the strong steric contact between the methyl substituent and the enamine moiety, the TS structure adopts a twisted boat conformation, substantially more energetic than the chair conformations adopted by all other TS structures in Figure 5. The energy difference between TS-19 and TS-22 is due to the axial orientation of the methyl substituent, while the energy difference between TS-25 and TS-22 is due to the axial orientation of the enamine moiety.

The detailed discussion made for the cyclization of compound **6** also applies to compound **7**. Thus, the *anti* structures are slightly more stable but, once again, this reaction pathway is not able to produce the enamine needed for the cyclization step (Scheme 6). As before, the reactive pathway has to proceed via the *syn* structures that originate two diastereomers of enamine **23**, in *syn/anti* conformational equilibrium (Scheme 6). As discussed for the cyclization of **6**, the rate-limiting step can be either the immonium formation or the initial attack of the proline molecule to the dialdehyde structure. For compound **7**, the immonium formation has slightly higher energy, and preferentially yields enamine **23** (*SSR*) in a relation of 61.8:38.2.

The rate-limiting step in Scheme 6 (TS-29) has an energy twice as high as that calculated for the cyclization step (45.14 kJ mol⁻¹), implying that enamines **23** shall react via two independent pathways, yielding eight possible products (Scheme 6 and Figure 6). The relative energy values and selectivities, calculated for the proline-catalyzed cyclization of compound **7**, are given in Table 6 and four selected structures are presented in Figure 6 (extra data is available

SCHEME 6. Proposed Mechanism for the Intramolecular Aldol Reaction of Dialdehyde 7 Catalyzed by (S)-Proline^a


^aFree energies in kJ mol^{-1} . The scheme shows only the TS structures, in order to be simplified. Extra data is in Supporting Information.

in Supporting Information). In Table 6, the values in italic were calculated considering the immonium formation as the rate-limiting step of the overall reaction, whereas the values in plain text were calculated considering that the selectivity results only from the cyclization step.

In contrast to the other calculated systems, the theoretical results obtained for compound **7** do not agree with the experimental data, as our calculations predict the formation

(37) List's paper does not state on what basis the stereochemical assignment was made. Thus, the absolute configurations we present in this manuscript are theoretical predictions.

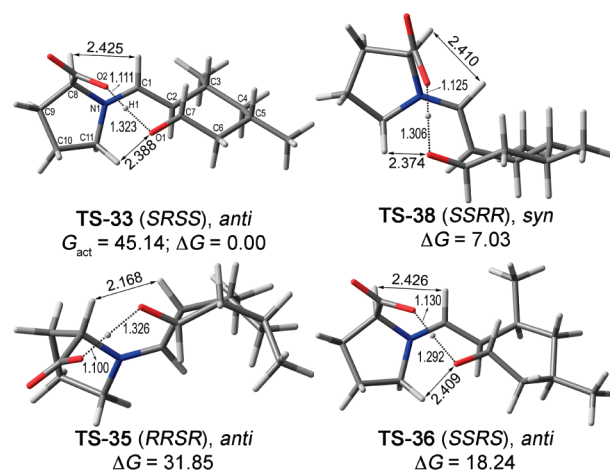


FIGURE 6. Calculated transition-state structures for the cyclization of **7** to **13** catalyzed by (S)-proline. Relative transition-state Gibbs energies (sf = 0.6395) in dichloromethane (kJ mol^{-1}).

TABLE 6. Relative Transition-State Gibbs Energies (kJ mol^{-1} , sf = 0.6395), Enantioselectivities, and Diastereoselectivities in the Intramolecular Aldol Reaction of Dialdehyde **7**, in Dichloromethane^a

transition state	B3LYP/6-31++G**// B3LYP/6-31G** (sf = 0.6395)		ref 10		
	ΔG (kJ mol^{-1})	ee (%)	dr (%)	ee (%)	dr (%)
TS-33 (SRSS) anti	0.00	74.7	43.5		
TS-34 (RSRR) anti	12.73, 5.69	98.8	93.9	75	50
TS-35 (RRSR) anti	31.85	100.0	0.6		
TS-36 (SSRS) anti	18.24, 11.21	99.2	0.1		
TS-37 (RRSS) syn	14.24	99.6	55.0		
TS-38 (SSRR) syn	7.03, 0.00	89.7	5.8	99 (anti)	50 (anti)
TS-39 (SRSR) syn	14.82	79.2	0.9		
TS-40 (RSRS) syn	17.43, 10.4	48.3	0.3		

^aWith (italic) and without (plain text) accounting for the selectivity obtained in **TS-29** (syn dr = 61.8:38.2).

of a mixture of diastereomers *syn* and *anti*, while the experimental data reports only the formation of *anti* products.³⁷ It is important to emphasize that, with the exception of this system, the theoretical results fit quite well with the experimental data and are in line with all the other previously discussed results. Thus, the activation energy for the cyclization was calculated as the lowest value ($45.14 \text{ kJ mol}^{-1}$) among all the studied structures, indicating that the presence of the two methyl groups strongly induces the proper conformation for the cyclization. The analysis of the eight possible TS structures also suggests that they behave in a similar way as those previously discussed, with the electrostatic contact between O1 and HC11 controlling the enantioselectivity and several steric contacts controlling the diastereoselectivity. The most stable TS structure is **TS-33**, since it is the only structure keeping the O1-HC11 electrostatic contact as well as the enamine moiety and the two methyl groups in equatorial position. Structure **TS-38** displays the second lowest activation energy in the set, as it only differs from structure **TS-33** in the axial position of its enamine group. All other structures are at least 12.7 kJ mol^{-1} higher energetic than **TS-33** and account with only 1.7% for the overall selectivity.

A special comment has to be made in respect to **TS-35** and **TS-36**. In order to fit the experimental data (dr = 50:50, *anti*

products only), one of these two structures should have an activation energy similar to that calculated for structure **TS-33**. At the same time, the energy of **TS-38** should be higher, in order to reduce its contribution to the final selectivity. By the analysis of all structures, we do not find a reason to justify a strong energy increase in structure **TS-38** (such a behavior would be in contrast to the rest of our data), and we also do not envisage how structures **TS-35** or **TS-36** could have lower energy, as their conformations are extremely distorted in order to reduce the steric contacts with the methyl groups. This means that the theoretical results are coherent and fit the experimental numbers if we consider a *syn:anti* 50:50 mixture of diastereomers. In fact, if we consider very low selectivity in the immonium formation step, then the calculated values (ee = 83.2, 99.3% and dr = 54.4:45.6) totally fit the experimental result, but keeping the *syn:anti* relation. In other words, the enamine formation is mandatory for the final selectivity, allowing for low diastereomeric ratios, but we do not find any explanation for the formation of only *anti* products. Thus, we believe that the abnormal experimental result has to be related to some experimental issue, which we are not able to rationalize with our theoretical data.

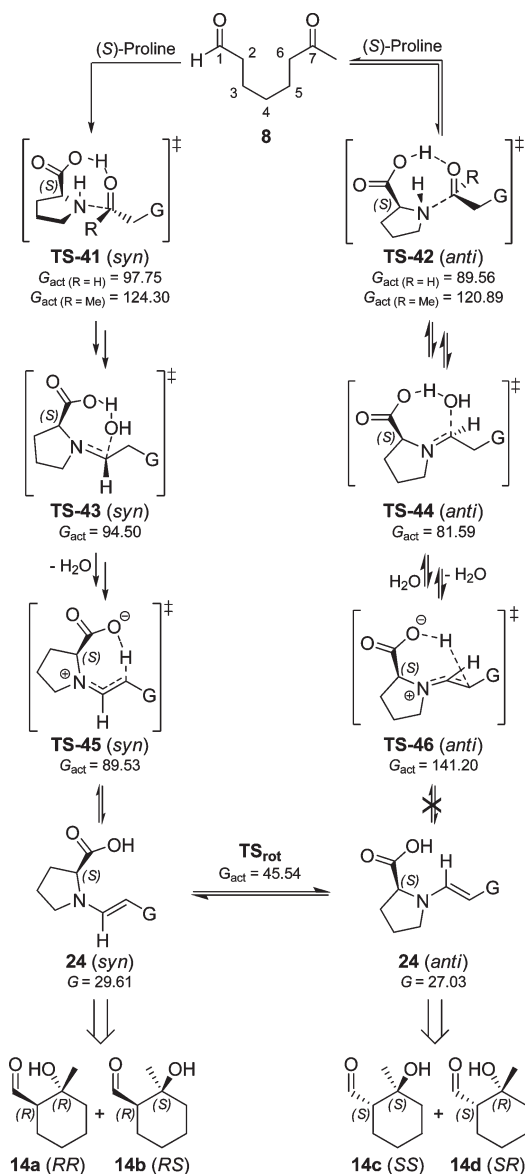
The experimental data obtained for the cyclization of compound **8** (7-oxo-octanal) indicates that it reacts only via enamine formation at the aldehyde side (Table 1 and Scheme 7). As a result, only two diastereomeric pairs of aldehyde **14** are formed (Table 1).¹⁰ This data is in agreement with our theoretical values (Scheme 7), as the proline attack at the ketone carbonyl group has higher activation energy (> 20 kJ mol⁻¹). The main reasons for this difference are the less electropositive carbon in the ketone carbonyl group relative to the aldehyde and, to a less extent, the larger steric effects observed in the attack at the ketone group.

As discussed for the cyclization of structures **6** and **7**, the *anti* pathway (via **TS-42**) does not allow for the formation of enamine **24**, and thus the reaction has to proceed via the *syn* pathway. Enamine **24** reacts via four possible TS structures, to form the cyclic intermediates. The relative energies of these transition states are given in Table 7, and Figure 7 shows the respective 3D transition-state structures.

The four structures in Figure 7 are, in all aspects, very similar to the structures in Figure 2. The same statement can be made for the relative activation energies. Nevertheless, the absolute activation energies for the cyclization of compound **8** are substantially higher (around 34 kJ mol⁻¹), because of the reasons discussed above for the initial attack of the proline molecule: larger steric contacts and less electropositive carbonyl group. These effects can also be observed in the relative bond lengths of the carbon-carbon forming bonds, which are considerably larger in the TS structures in Figure 7 than in all other studied structures.

The higher activation energy obtained for the cyclization of **8** makes it the rate-limiting step of the reaction, in contrast to the two previous discussed systems. This is not relevant for the calculation of the final selectivity, as there is no selectivity induction before the cyclization. Nevertheless, it is an interesting result, as it shows that it is not possible to generalize on the rate-limiting step of all types of aldol cyclizations. This different behavior results from the special case of enamine formation at a reactive aldehyde carbonyl group, whereas in the cyclization step the attack occurs at a less reactive ketone carbonyl group, as discussed above.

SCHEME 7. Proposed Mechanism for the Intramolecular Aldol Reaction of Dialdehyde **8** Catalyzed by (*S*)-Proline^a



^aFree energies in kJ mol⁻¹. The scheme only shows the TS structures, in order to be simplified. Extra data is in Supporting Information.

TABLE 7. Relative Transition-State Gibbs Energies (kJ mol⁻¹, sf = 0.6395), Enantioselectivities, and Diastereoselectivities in the Intramolecular Aldol Reaction of Ketoaldehyde **8**, in Dichloromethane

transition state	B3LYP/6-31++G**// B3LYP/6-31G** (sf = 0.6395)		ref 10		
	ΔG (kJ mol ⁻¹)	ee (%)	dr (%)	ee (%)	dr (%)
TS-47 (SS) <i>anti</i>	0.0	98.1	65.7	99	66.7
TS-48 (RR) <i>anti</i>	11.46				
TS-49 (RS) <i>syn</i>	8.48	87.6	34.3	95	33.3
TS-50 (SR) <i>syn</i>	1.74				

The main differences between the relative activation energies in the cyclization of compounds **3** and **8** are a result of the relative orientation of the ketone methyl group and the enamine moiety in **TS-47** to **TS-50** (Figure 7). In structures **TS-47** and **TS-48** these two groups are in *gauche* conformation,

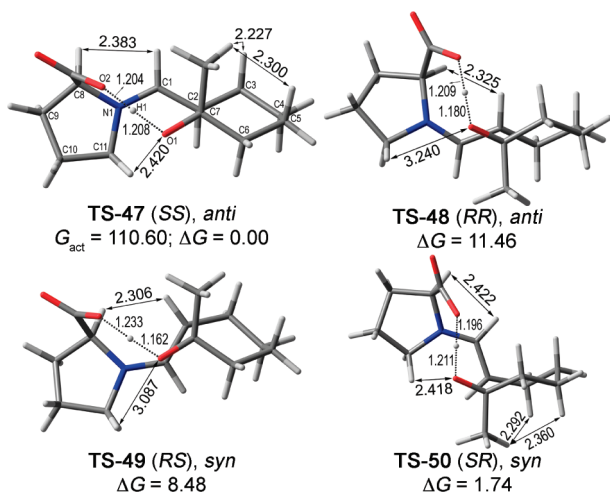


FIGURE 7. Calculated transition-state structures for the cyclization of **8** to **14** catalyzed by (*S*)-proline. Relative transition-state Gibbs energies (sf = 0.6395) in dichloromethane (kJ mol^{-1}).

whereas in structures **TS-49** and **TS-50** they adopt the *anti* conformation. All other interactions are similar to those described for structures **TS-1** to **TS-4** (Figure 2), resulting in similar energy differences between **TS-48** and **TS-47** ($11.46 \text{ kJ mol}^{-1}$) and **TS-2** and **TS-1** ($11.27 \text{ kJ mol}^{-1}$), as well as between **TS-50** and **TS-49** (6.74 kJ mol^{-1}) and **TS-4** and **TS-3** (6.37 kJ mol^{-1}). Thus, in the two systems the predicted enantioselectivity is similar, in agreement with the experiment. On the other hand, the *gauche* orientations between the methyl and the enamine groups in structures **TS-47** and **TS-48** slightly increase their activation energies (around 4 kJ mol^{-1}) relative to structures **TS-49** and **TS-50**, thus originating a reduction in the calculated diastereoselectivity, well in agreement with the experimental values.

Conclusions

The empirical transition-state model proposed by List for the intramolecular aldol reaction of substituted 1,7-dicarbonyl compounds catalyzed by (*S*)-proline was theoretically analyzed with quantum chemical calculations. In order to obtain good agreement between our calculated values and the experimental data, we found it necessary to use a solvent model (PCM) together with a basis set with included diffuse functions (6-31++G**). The theoretical data confirm that the main factors contributing for the reaction selectivity in the cyclization step are of steric and electrostatic nature, in agreement with our previous rationalization. Nevertheless, for dialdehydes that can originate two diastereomeric enamine intermediates, any of the reaction steps that precede the cyclization can also be of major importance in the rationalization of the final reaction selectivity. The theoretical data

agrees in good extension with List's experimental results, both in enantioselectivity and diastereoselectivity, with only a single exception. However, even in this situation we could show that the calculated values fit quite well with the experimental data, if instead of a mixture of *anti* diastereomers we consider a mixture of *syn/anti* structures. Because of the high consistency of the theoretical data and the excellent agreement with the experimental results, we believe that the apparent failure in one of the analyzed systems is probably a result of experimental issues and not of a less appropriated theoretical model.

Computational Methods

All calculations were performed using density functional theory (DFT)³⁸ with the Gaussian 03, Revision E.01 software package.³⁹ The geometries of all stationary points were full optimized with the B3LYP functional and the 6-31G** basis set, and their nature (minimum or transition state) was determined by frequency analysis. Zero-point energies and thermal corrections, at 25 °C, have been taken from unscaled vibrational frequencies. Reported activation energies include zero-point and thermal corrections. The effect of solvent on the energies was studied by single-point calculations at the B3LYP/6-31++G** level of theory. The polarizable continuum model (PCM)⁴⁰ was used together with UAKS radii and the dielectric constant of dichloromethane (DCM). All bond lengths are in angstroms (Å), and the energies are in kJ mol^{-1} . Activation energies are calculated relative to the reagents.

Acknowledgment. We are grateful to the Fundação para a Ciência e Tecnologia (SFRH/BD/17547/2004 and PTDC/QUI-QUI/104056/2008) for financial support.

Supporting Information Available: Extra TS structures with respective activation energies, Cartesian coordinate matrixes and electronic energies of all calculated structures. This material is available free of charge via the Internet at <http://pubs.acs.org>.

(38) Parr, R. G.; Yang, W. *Density Functional Theory of Atoms and Molecules*; Oxford University Press: Oxford, 1989.

(39) Frisch, M. J.; Trucks, G. W.; Schlegel, H. B.; Scuseria, G. E.; Rob, M. A.; Cheeseman, J. R., Jr.; J. A. M.; Vreven, T.; Kudin, K. N.; Burant, J. C.; Millam, J. M.; Iyengar, S. S.; Tomasi, J.; Barone, V.; Mennucci, B.; Cossi, M.; Scalmani, G.; Rega, N.; Petersson, G. A.; Nakatsuji, H.; Hada, M.; Ehara, M.; Toyota, K.; Fukuda, R.; Hasegawa, J.; Ishida, M.; Nakajima, T.; Honda, Y.; Kitao, O.; Nakai, H.; Klene, M.; Li, X.; Knox, J. E.; Hratchian, H. P.; Cross, J. B.; Bakken, V.; Adamo, C.; Jaramillo, J.; Gomperts, R.; Stratmann, R. E.; Yazyev, O.; Austin, A. J.; Cammi, R.; Pomelli, C.; Ochterski, J. W.; Ayala, P. Y.; Morokuma, K.; Voth, G. A.; Salvador, P.; Dannenberg, J. J.; Zakrzewski, V. G.; Dapprich, S.; Daniels, A. D.; Strain, M. C.; Farkas, O.; Malick, D. K.; Rabuck, A. D.; Raghavachari, K.; Foresman, J. B.; Ortiz, J. V.; Cui, Q.; Baboul, A. G.; Clifford, S.; Cioslowski, J.; Stefanov, B. B.; Liu, G.; Liashenko, A.; Piskorz, P.; Komaromi, I.; Martin, R. L.; Fox, D. J.; Keith, T.; Al-Laham, M. A.; Peng, C. Y.; Nanayakkara, A.; Challacombe, M.; Gill, P. M. W.; Johnson, B.; Chen, W.; Wong, M. W.; Gonzalez, C.; Pople, J. A. *Gaussian 03, Revision E.01*; Gaussian, Inc.: Wallingford, CT, 2004.

(40) Cossi, M.; Scalmani, G.; Rega, N.; Barone, V. *J. Chem. Phys.* **2002**, *117*, 43–54.